AD-A035 881 NAVAL UNDERWATER SYSTEMS CENTER NEW LONDON CONN NEW --ETC F/G 17/1
PROPAGATION LOSS MEASUREMENTS AT 400 HERTZ IN THE BIFI RANGE US--ETC(U)
JAN 71 W G KANABIS

UNCLASSIFIED NUSC/NL-TM-2211-26-71 NL

| OF |
AD
AD35881

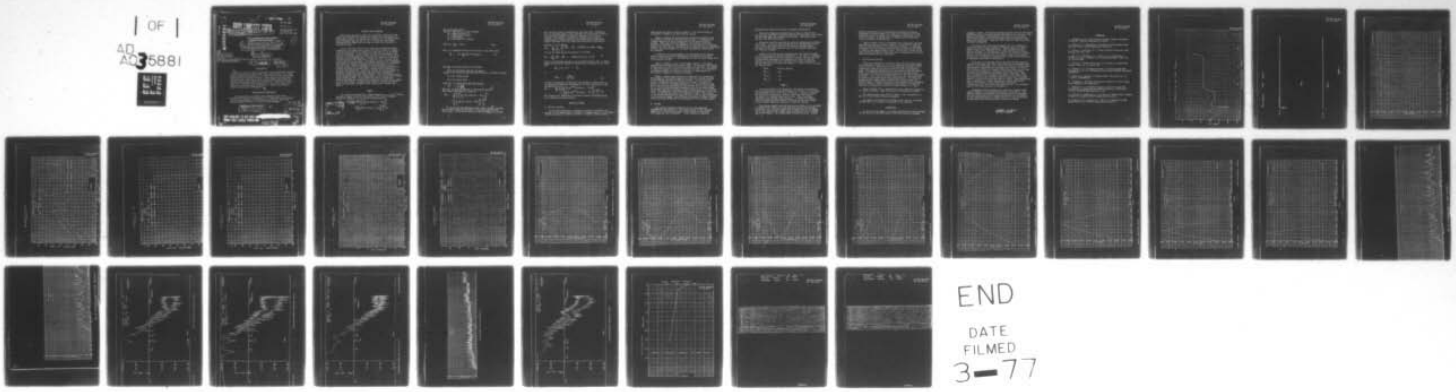

END

DATE
FILMED
3-77

NAVAL UNDERWATER SYSTEMS CENTER
NEWPORT, RHODE ISLAND 02840

(6) (9) Technical + memo.)

(1) B.S.

PROPAGATION LOSS MEASUREMENTS AT 400 HERTZ IN THE BIFI RANGE USING A TOWED SOURCE.

by

(10) William G. Kanabis

(16) F11552

(17) SF11552001

NUSC/NL Technical Memorandum No. 2211-26-71

(11) 27 Jan[illegible]71

(12) 33p.

INTRODUCTION

This is a report on 400 Hz propagation loss measurements conducted between 25 March and 18 April 1969. These tests are part of a series using the BIFI Range (Reference 1) located between Block Island, Rhode Island and Fishers Island, New York. Three types of acoustic tests were performed, consisting of fixed range-variable depth pulsed CW, variable range-variable depth CW and pulsed CW. The object of these tests was to determine the propagation loss of a 400 Hz signal as a function of range and depth of the source. Depths were chosen to enhance various modes of propagation.

ADMINISTRATIVE INFORMATION

This memorandum was prepared under NUSC/NL Project Title: Shallow Water Acoustic Investigation, W. R. Schumacher and B. Sussman, Principal Investigators. The sponsoring activity was Naval Ship Systems Command, Code OOV1, J. Reeves, Program Manager.

ACOUSTIC TEST PROCEDURE

Three types of acoustic tests were conducted. During all tests signals were received by a hydrophone located at point B, Figure 1, near Fishers Island. The signals were generated by a Honeywell 400 Hz source suspended from the USL "O" Boat. During all tests bathythermograms were taken along the range and were later converted to velocity profiles.

In the first test (Test A) the source Boat transmitted signal sequences of 45 seconds on-15 seconds off for ten minutes at a depth of 60 feet from each of 10 stations at ranges from 1.6 to 13.2 miles from the hydrophone. In the second test (Test B) the projector was towed at a constant speed at a depth of about 75-80 feet while 400 Hz CW signals were being generated. CW runs were conducted on 26 March when the projector was towed from a range of 6.3 to 1.3 miles and on 1 April from 9.1 to 0.6 miles. All signals received by the hydrophone near Fishers Island were transmitted to the Laboratory by a telephone line data link. There the signals were passed through a filter centered at 400 Hz with a bandwidth of 50 Hz and their envelope level recorded digitally on punched cards. Program S1298 (Reference 2) processed the pulsed data. During the CW runs the received signal was recorded continuously on punched cards which were subsequently processed through the Univac 1108 computer. Plots of propagation loss versus range and signal level versus range for the CW runs were obtained on the CalComp plotter. In the third test (Test C) pulses 100 milliseconds long were transmitted at depths of 58 and 86 feet at ranges of 3, 4, and 5 miles. A Sanborn paper recorder recorded the signals after they had passed through a filter whose center frequency was 400 Hz.

THEORY

The sound field produced by a simple harmonic source in a two-layered half-space (Figure 2) with a free surface at z=0 and the boundary between two fluids at z = h is given by (Reference 3):

$$\frac{\sin(\omega t + \phi)}{\omega^2 \sqrt{r}} \left\{ \left[\sum_m P_m \cos(k_m r - \pi/4) \right]^2 + \left[\sum_m P_m \sin(k_m r - \pi/4) \right]^2 \right\}^{1/2} \quad (1)$$

for large ranges ($kr >> 1$)
where $w = 2\pi f$ and f is the frequency
Φ = phase function of w
r = distance from source
m = mode number
Km = horizontal wave numbers

where $Km = \frac{W}{C} \sin\theta$ (1a)

Where θ is measured relative to the normal to the bottom and

$$P_m = p_m \frac{1}{\rho_s} \varphi_m(z) \varphi_m(z_o) \quad (2)$$

where ρ_s is the layer density at the source

p_m is the excitation function for mode m.
$\varphi_m(z)$ is the normalized amplitude distribution as a function of depth

Z is the receiver depth

Zo is the source depth

Since Φ is defined such that the pressure

$$P = -\rho \frac{\partial^2 \Phi}{\partial t^2} \quad (3)$$

where ρ is the layer density at the receiver position
the pressure amplitude pa is given by

$$p_a = \frac{\rho}{r} \left\{ \left[\sum_m p_m \cos(k_m r - \pi/4) \right]^2 + \left[\sum_m p_m \sin(k_m r - \pi/4) \right]^2 \right\}^{1/2} \quad (4)$$

It can be seen from Equations 2 and 4 that, once φ_m is known, one can easily determine the effect of the source depth on the sound field. If the source depth z_o is such that $\varphi_m(z_o)$ is a node,

then the mode m will be suppressed in the sound field. Similarly, if z_o is such that $\varphi_m(z_o)$ is an antinode, the sound field of mode m will be greater than at any depth for which $\varphi_m(z_o)$ is not an antinode. The ability to eliminate or enhance a given mode by manipulating the source depth has been demonstrated in model tank studies (Reference 4) and in large scale experiments (Reference 5).

Equation 4 can be written

$$P_n = \frac{\rho}{r\pi} \sum_{n \neq m} \sum_{m} \left(P_m^2 + P_n^2 + 2 P_m P_n \cos(r(k_m - k_n)) \right) \quad (5)$$

If only two modes are excited equation (5) becomes

$$P_n = \frac{\rho}{r\pi} \left(P_i^2 + P_j^2 + 2 P_i P_j \cos(r(k_i - k_j)) \right) \quad (6)$$

Thus, an interference pattern is set up between modes i and j in which maxima and minima are spaced one interference wavelength, Λ_{ij}, apart, and

$$\Lambda_{ij}(k_i - k_j) = 2\pi$$

or

$$\Lambda_{ij} = \frac{2\pi}{k_i - k_j} \quad (7)$$

For small attenuation of individual modes Equation 7 may be used to calculate the interference wavelength of two modes and Equation 4 may be rewritten as

$$P_n = \frac{\rho}{r\pi} \left\{ \left[\sum_m P_m e^{-\delta_m r} \cos(k_m r - \pi/4) \right]^2 + \left[\sum_m P_m e^{-\delta_m r} \sin(k_m r - \pi/4) \right]^2 \right\}^{1/2} \quad (8)$$

USL Program S1441 (Reference 6) provides solutions for $\varphi_m(z)$ and k_m for an arbitrary velocity profile.

RESULTS OF TESTS

A. Discrete Stations

As previously described, a sequence of signals 45 seconds on -15 seconds off was transmitted at 10 stations at ranges from 1.6 to 13.2 miles with the projector at a depth of 60 feet. A typical velocity profile

taken during the tests is shown in Figure 3. The sound velocity in the bottom is assumed to be 5700 feet per second.

Figure 4 presents the experimentally determined propagation loss as a function of range for the fixed station case. In addition, the standard deviation of the 10 long pulses at each range station is plotted. These data are then compared to the Colossus theoretical predictions (Reference 7). The agreement is fairly good; it is apparent, however, that the Colossus predictions do not take into account oscillation in level versus the range, i.e. the modal interference effects which are observed.

A comparison between propagation loss determined by the average level of each pulse and that determined by the peak level of each pulse is shown in Figure 5. The difference of the two losses ranges from 3 to 6 dB over the run.

Figure 6 presents a plot of the average variance of the signal measured over individual pulses versus range. At each range the variance of the envelope of each of 10 received pulses was computed. The average of these ten values is plotted as a function of range. It is difficult to determine whether the extreme fluctuations in measurements are the result of temporal or spatial variations.

Figure 7 compares the variances of propagation loss measured by the average and the maximum signal levels over the 10 pulses recorded at each station, plotted as functions of range. At each range the value of propagation loss was computed in two ways for each of 10 pulses. In the first procedure propagation loss was calculated using the average value of the envelope of the received pulse as the received level. In the second procedure propagation loss was calculated using the maximum value of the envelope of the received pulse as the received level. The variances of the 10 propagation loss measurements using each of the two methods are plotted as a function of range. The variance of the maximum measurements is less than that of the average measurements at all except one range. The difference is greatest at ranges in which there were large fluctuations in the amplitude of the received signal.

B. CW Runs

The velocity structure during CW runs over the range was approximately as in Figure 3. The sound velocity in the bottom was assumed to be 5700 feet per second and the density of the bottom 2.00 grams per cubic centimeter. These figures are based on

geological data taken from the area considered (Reference 8).

Theoretical amplitude distributions are shown in Figures 8-11 for the first four modes of sound as functions of depth for a flat bottom - 160 feet deep under the conditions stated above. The figures were obtained from USL Program S1441.

During the runs the projector was towed at approximately mid-depth (75-80 feet). It can be seen from Figures 8-11 and Equations 2 and 4 that at this depth modes two and four should be somewhat damped and modes one and three should be close to their maximum amplitudes as a function of depth.

Figures 12-15 show the ray equivalents for the first four modes of the distributions appearing in Figures 8-11. The angle of incidence of the propagating ray upon the bottom Θ_b is shown. One can calculate the horizontal wavenumber Km from Equation 1a knowing Θ_b and the velocity of sound in the water just above the bottom; then, Λ_{ij} for any two modes can be obtained from Equation 7. Table I shows $\Lambda_{1,2}$, $\Lambda_{1,3}$ and $\Lambda_{1,4}$ in miles.

Λ_{mn}	Distance (nmiles)
$\Lambda_{1,2}$	1.02
$\Lambda_{1,3}$	.39
$\Lambda_{1,4}$	.21

TABLE I

Plotted in Figure 16 is propagation loss versus range measured while the projector was towed at a depth of 75-80 feet. The sea state was approximately zero at the time of testing. A periodic variation in the loss is clearly seen. Distinct variations with period of the order of 0.3 nautical miles can be seen. These variations correspond approximately to $\Lambda_{1,3}$ and $\Lambda_{1,4}$. In order to determine more accurately the periodicity of the variations spectral analysis of the received signal as a function of range was employed.

The spectra computed from the data shown in Figure 16 are presented in Figures 17-19. Figure 17 is the spectrum computed from the auto-correlation function of the sample with a maximum lag of 1750 samples out of the total of 4480. Figure 18 is the same plot with a maximum lag of 3500 samples. USL Program S0855 provided the plots. A power

spectrum obtained by use of Program S1086 employing fast Fourier transforms is shown in Figure 19. Shown in all three plots are the frequencies which correspond to the interference wavelengths of the first four modes. It appears that the highest peaks in the power spectra correspond to $\Lambda_{1,2}$ and $\Lambda_{1,4}$.

Figure 20 gives a plot of propagation loss versus range measured while the projector was towed at a depth of about 80 feet. The sea state was approximately 2 or 3 at the time of testing. A comparison of Figures 16 and 20 indicates that the high sea state has the effect of obscuring any simple periodic effect. This result is shown in the power spectrum of Figure 21 where the peaks corresponding to the interference wavelengths do not predominate.

C. 100 Millisecond Pulses

Tests were conducted on 18 April in which 100 millisecond pulses were transmitted at range of 3, 4, and 5 miles and with source depths of 58 and 86 feet. The velocity profile appearing in Figure 22 was slightly more negative than the one present in the first previous tests. The amplitude distribution was calculated through USL Program S1441; it was found that node points existed for the second mode at a depth of 94 feet, for the third mode at 60 feet, and for the fourth at 86 feet. Thus, with the source 58 feet deep, the third mode would be damped and one would expect three dominant modes. At 86 feet the second and fourth modes would be damped and one would expect two dominant modes. The group velocity of a mode decreases with increasing order of the mode. Thus one would expect the modes to be separated with mode 1 arriving first followed in order by modes 2, 3, and 4.

Shown in Figure 23 is a representative pulse which was transmitted at a depth of 86 feet. There clearly are two predominant arrivals.

The representative pulse shown in Figure 24 was transmitted at a depth of 58 feet; three arrivals predominate.

The number of arrivals did not change as the range was increased, although there was a decrease in amplitude of the arrivals.

CONCLUSIONS

As can be seen in Figure 1, the tests described above were performed over the portion of the BIFI range in which the bottom is extremely

irregular in depth. The results obtained compared well with theoretical predictions for a flat bottom during conditions of low sea state. The measured interference wavelengths and the effect of the variation of the source depth on the received signal show good agreement with theoretical predictions. High sea states seemed to induce relatively incoherent propagation.

The results for low sea states suggest that it is feasible to divide the range into many segments of constant depth and compute signal levels from normal mode theory. This procedure has been used in reference 9. Furthermore, if normal mode theory holds in the most irregular part of the BIFI range it is reasonable to assume that it will be valid over the entire range. This is a necessary condition for the effective utilization of the BIFI normal mode array in experiments described in reference 10.

In general it is expected that as the range between source and receiver is increased the higher order modes will be attenuated more than the lower order modes. As a result the lower order modes become much greater in amplitude than the higher order modes. It can be seen in Figure 24 that at a range of three miles there does not seem to be severe attenuation of the higher order modes since there are three major arrivals approximately equal in amplitude. This lack of attenuation in the higher order modes can be attributed to the hard bottom in the vicinity of Fishers Island where the sound speed in the bottom is about 5700 feet per second. These observations will be compared in a future memorandum to similar measurements made in the vicinity of Block Island where the bottom is much softer than the bottom near Fishers Island. The operations plan for such tests is given in reference 11.

Propagation loss was measured as a function of range and the results compared to the Colossus predictions (reference 7). The agreement between the measured and predicted values of propagation loss was fairly good but the Colossus predictions did not account for the observed variation in signal level due to the interference between modes which were predicted by normal mode theory.

William G. Kanabis
WILLIAM G. KANABIS

REFERENCES

1. Schumacher, W. R. "Shallow Water Acoustic Studies; information concerning." NUSC/NLL Memorandum 2211-18-68.

2. Kanabis, W. G. "Description of Software of BIFI Automated Data Reduction System" NUSC/NL Memorandum 2211-91-69.

3. Tolstoy, I. and Clay, C. B. "Ocean Acoustics" McGraw-Hill Book Company, New York, 1966.

4. Eby, R. K., Williams, A. O., Ryan, R. P., and Tamarkin, P. "Study of Acoustic Propagation in a Two-Layered Model", JASA, Vol. 32, January 1960.

5. Tolstoy, I. "Shallow Water Test of the Theory of Layered Wave Guides", JASA, Vol. 30, April 1958.

6. Kanabis, W. G. "A Computer Program to Calculate Normal Mode Propagation over a Flat Homogeneous Ocean Bottom" NUSC/NLL Memorandum 2211-296-69.

7. Hasse, R. W "Colossus II Summary Report" USL Report No. 513, 3 July 61 (CONFIDENTIAL)

8. Gallagher, J. "Geologic and Acoustic Properties of Block Island Sound Sediments" (In Preparation)

9. Kanabis, W. G. "A Computer Program to Calculate Normal Mode Propagation in a Medium in which Stratification is a Function of Position" NUSC/NLL Memorandum 2211-11-71.

10. Sussman, B., Kanabis, W. G., and Arens, H. "Shallow Water Acoustic Studies; new schedule" NUSC/NL Memorandum 2211-16-71.

11. Kanabis, W. G., and Arens, H. "Tests to be Conducted on BIFI Range; Op Plans For" NUSC/NL Memorandum 2211-324-70.

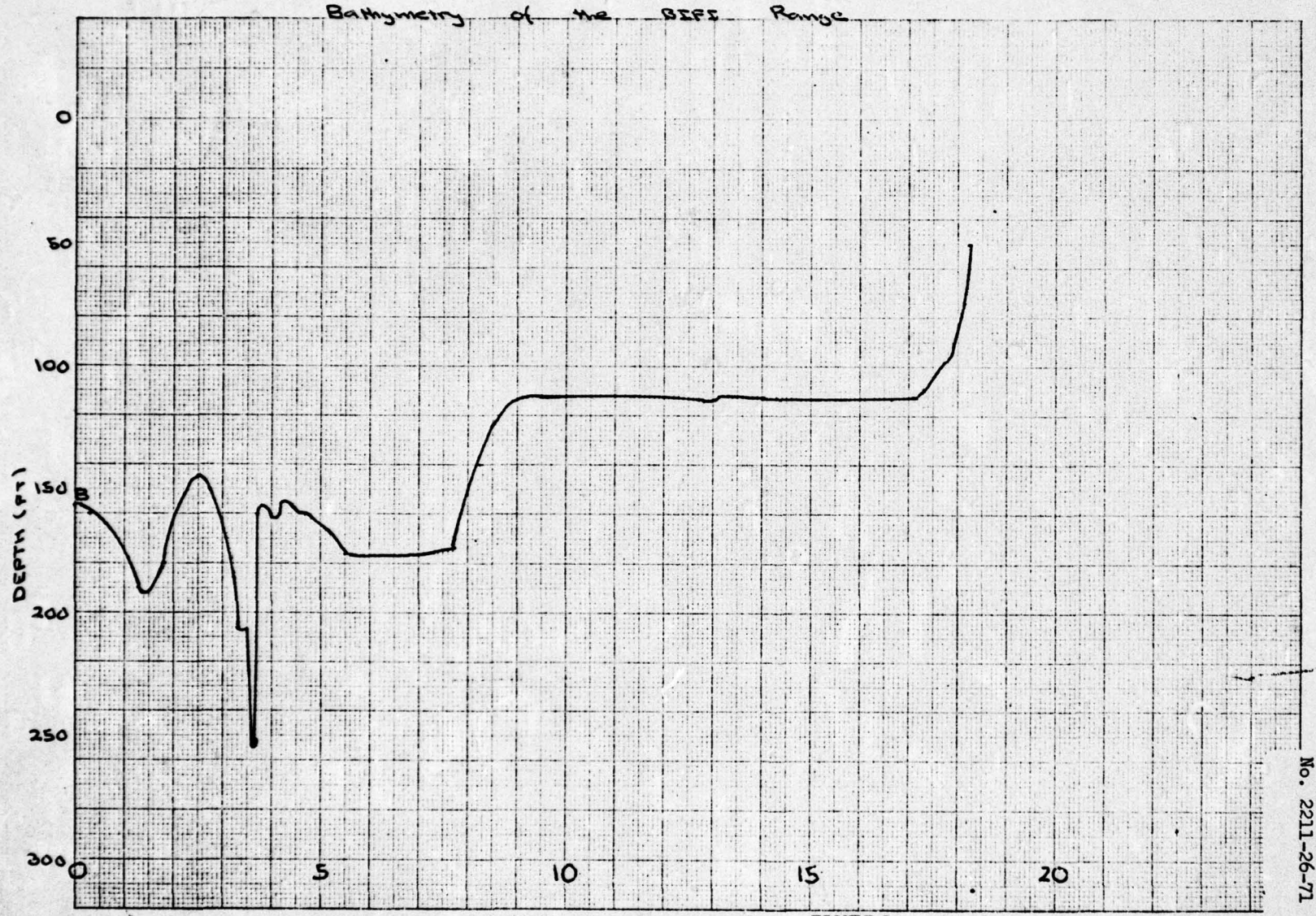

FIGURE 1

NUSC/NL Tech Memo
No. 2211-26-71

Two-layered Half Space

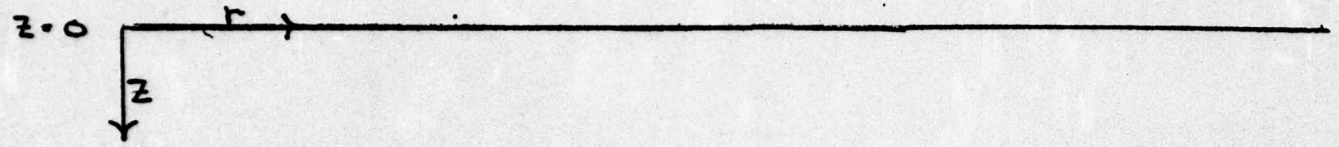

$\rho_1 c_1$

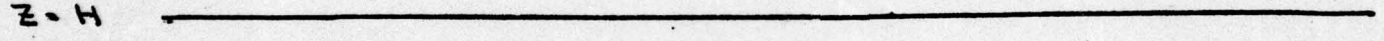

$\rho_2 c_2$

FIGURE 2

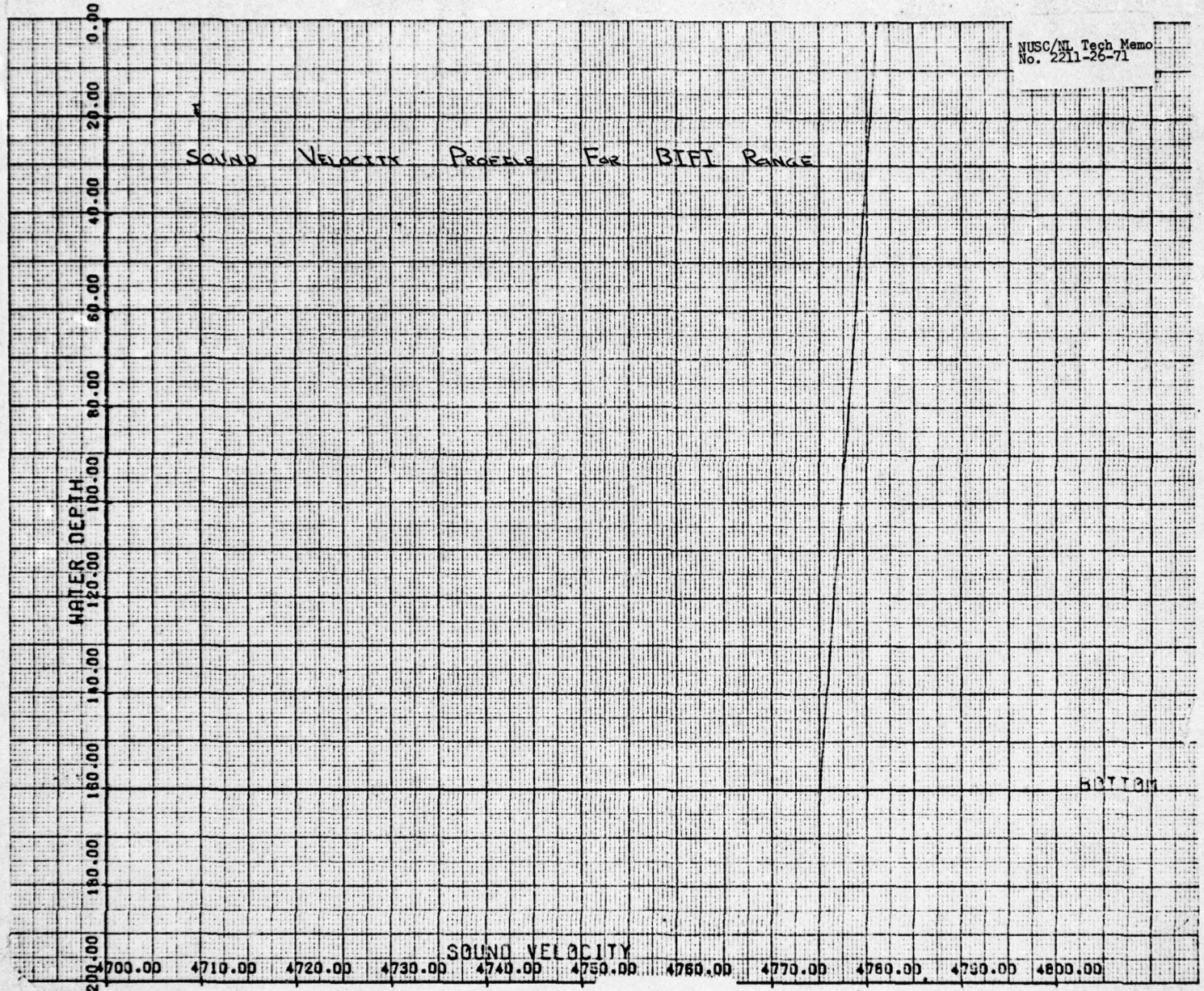

FIGURE 3

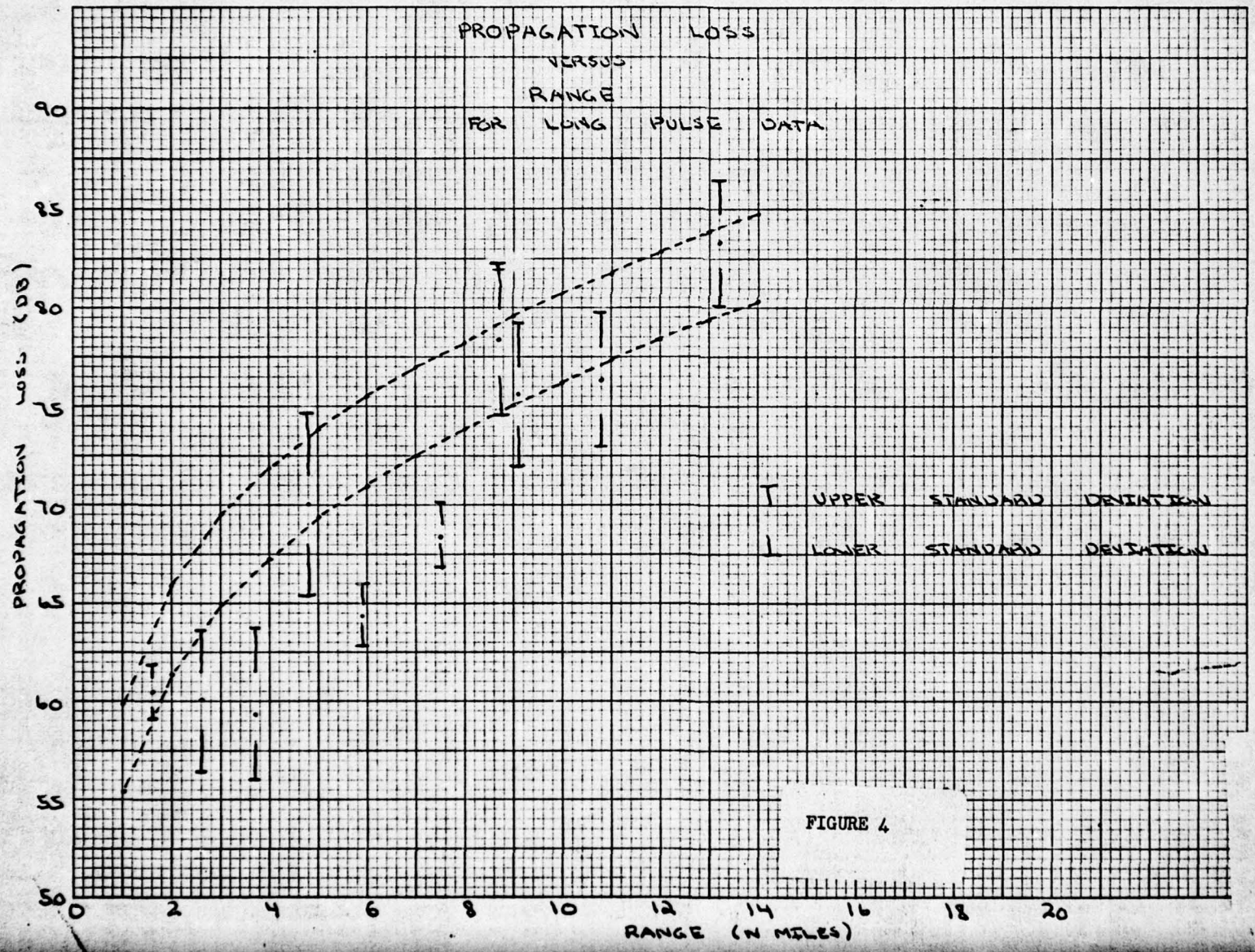

FIGURE 4

FIGURE 5

KEUFFEL & ESSER CO.

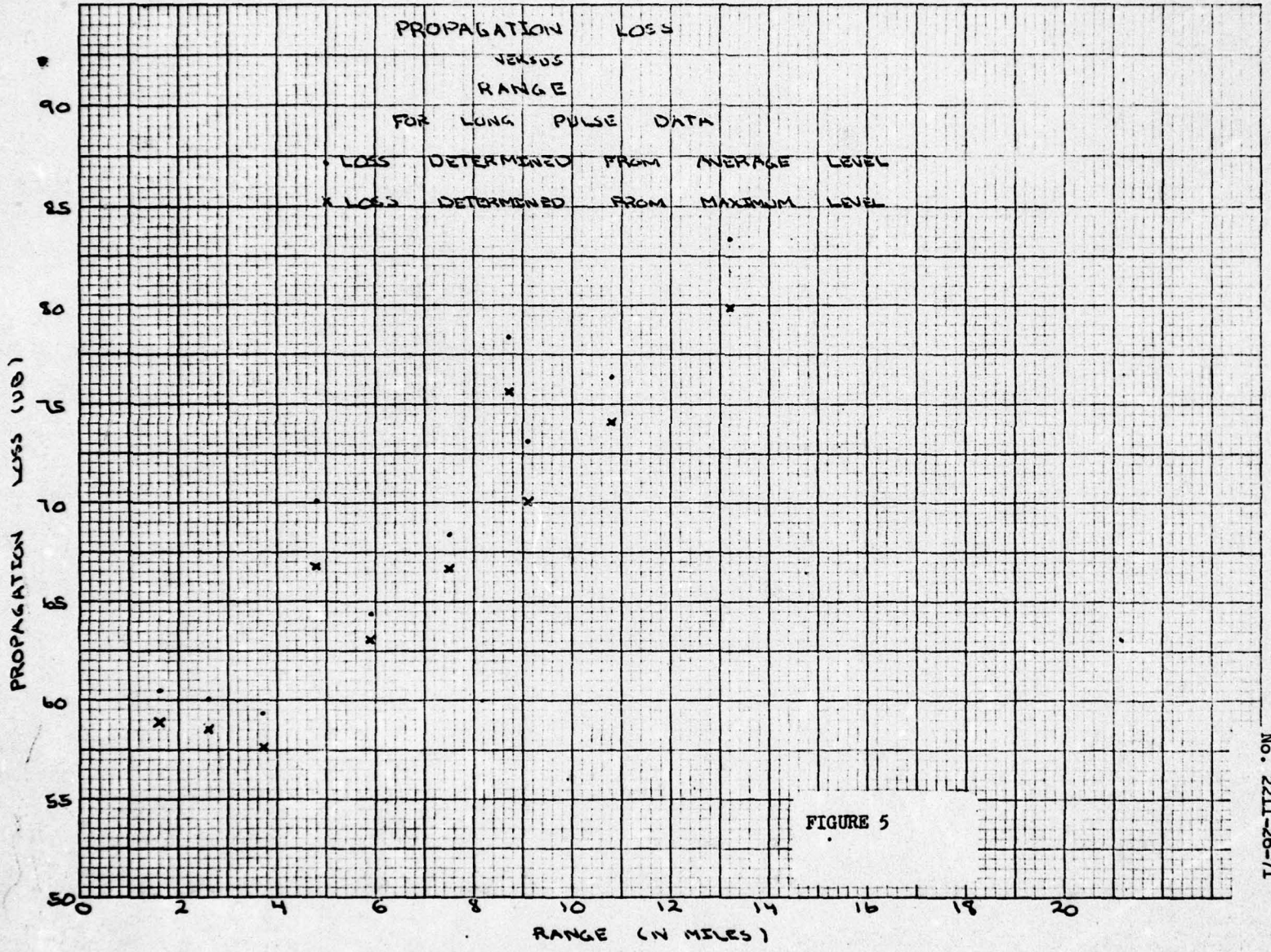

FIGURE 5

NUSC/NL Tech Memo
No. 2211-26-71

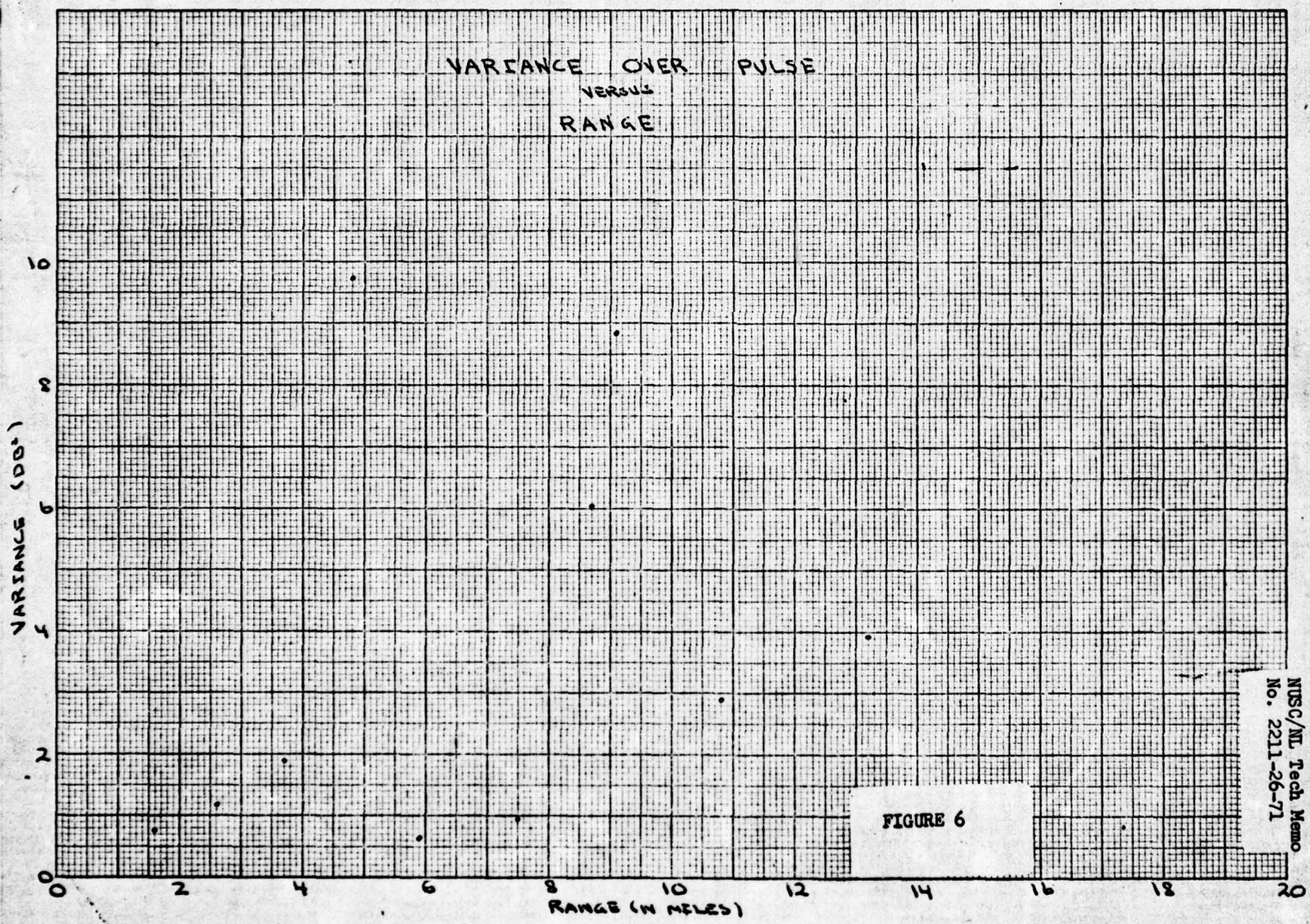

FIGURE 6

NUSC/NL Tech Memo
No. 2211-26-71

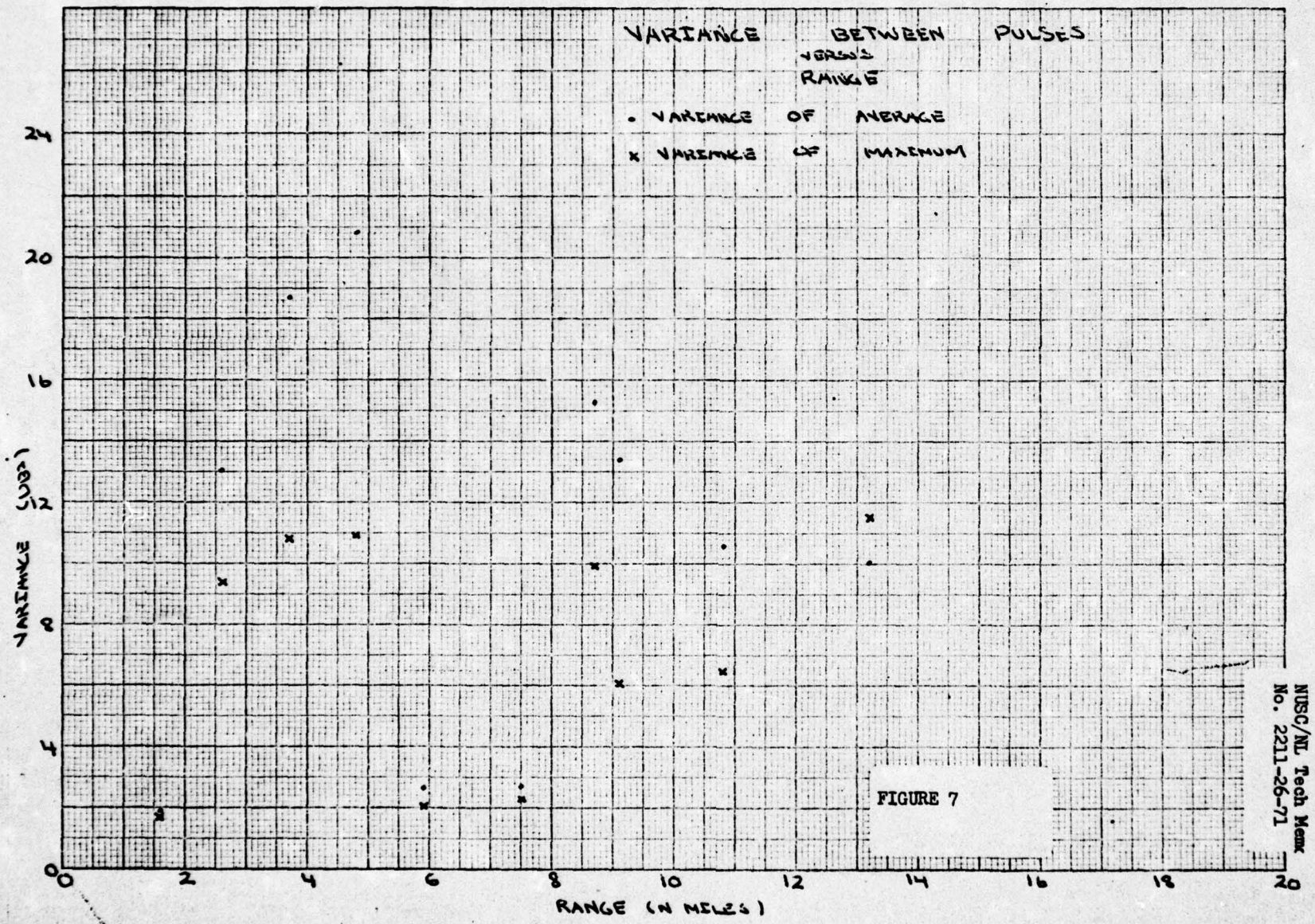

FIGURE 7

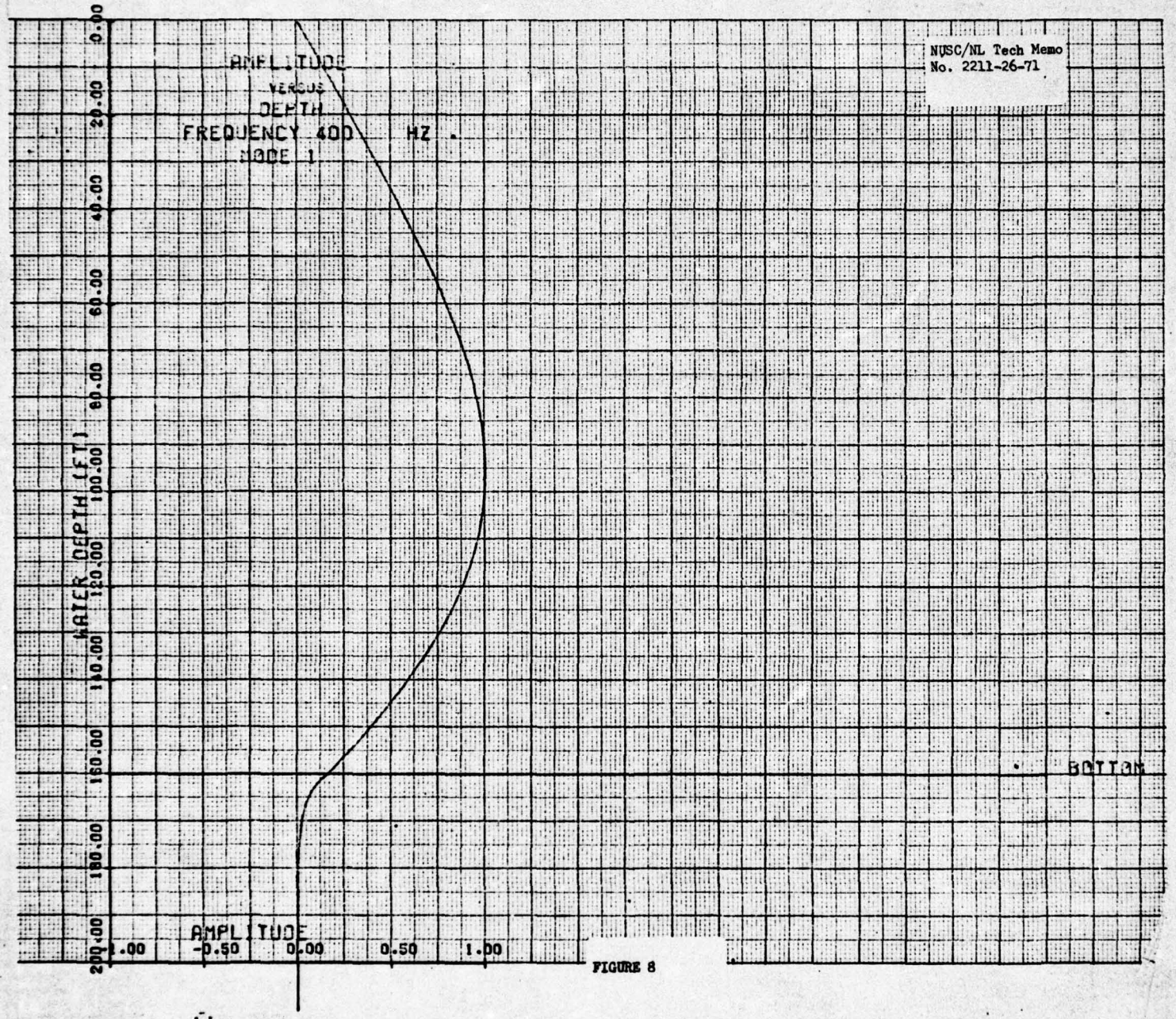

FIGURE 8

CALIFORNIA COMPUTER PRODUCTS, INC. ANAHEIM, CALIFORNIA CHART NO. 02 MADE IN U.S.A.

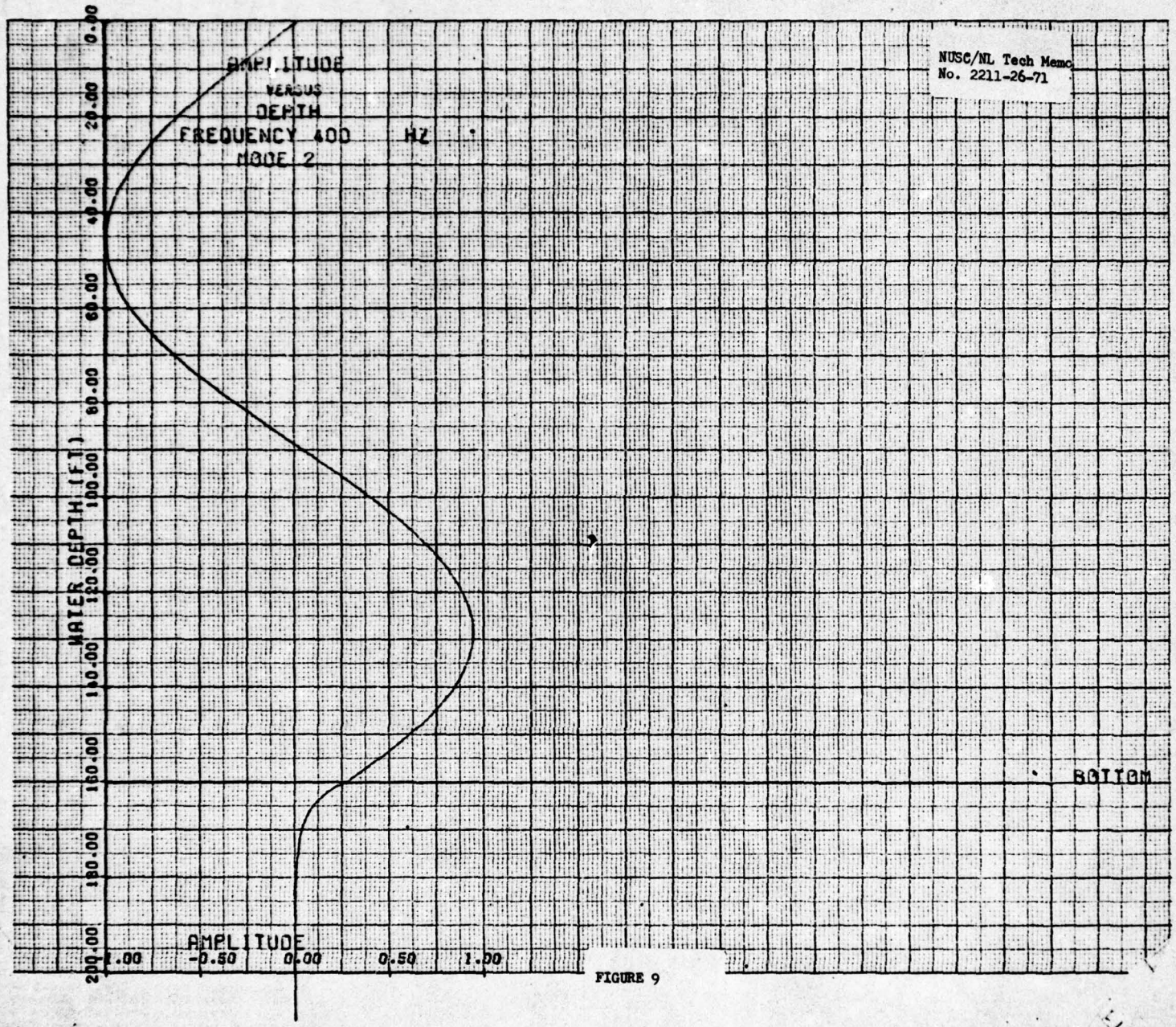

FIGURE 9

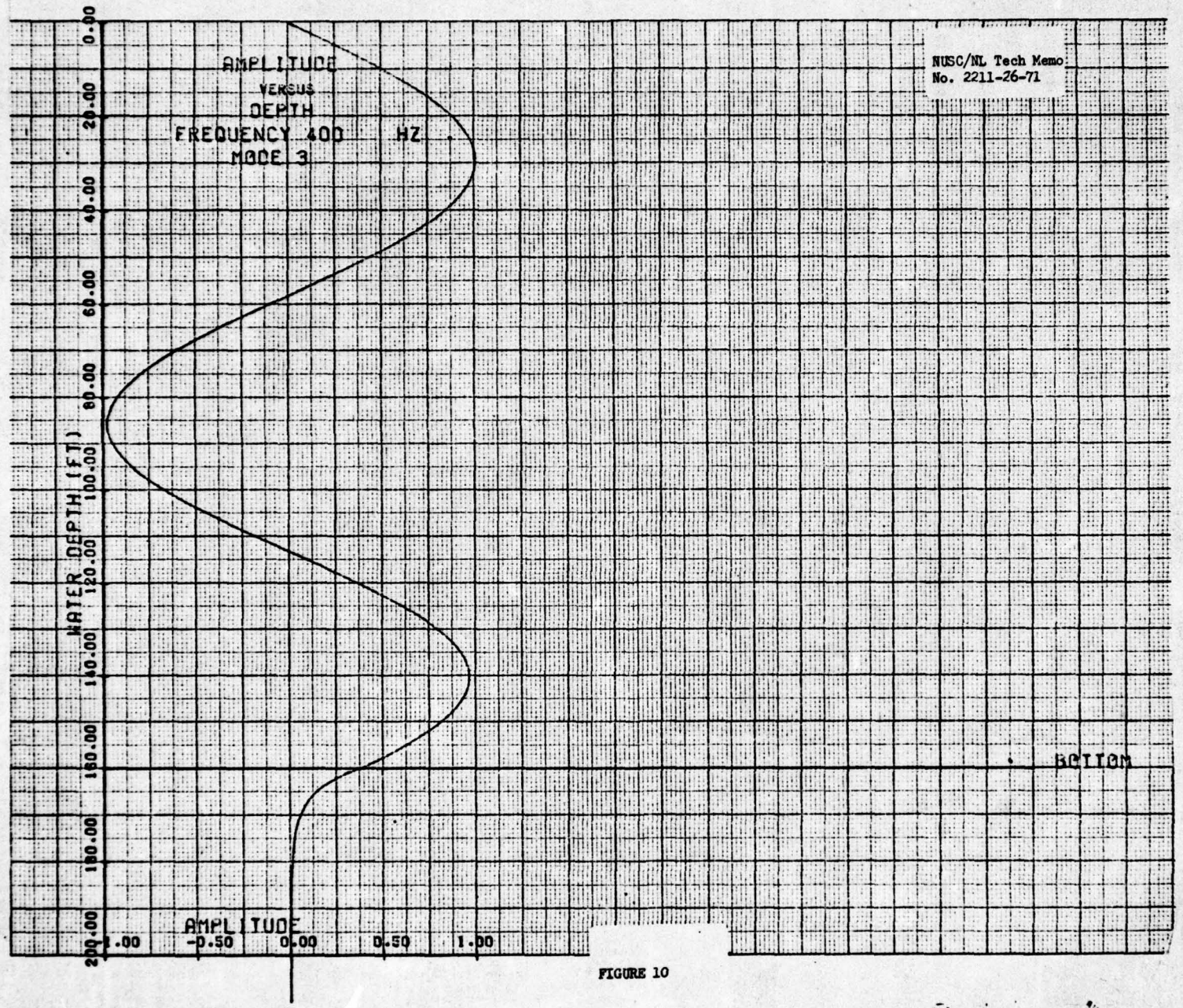

FIGURE 10

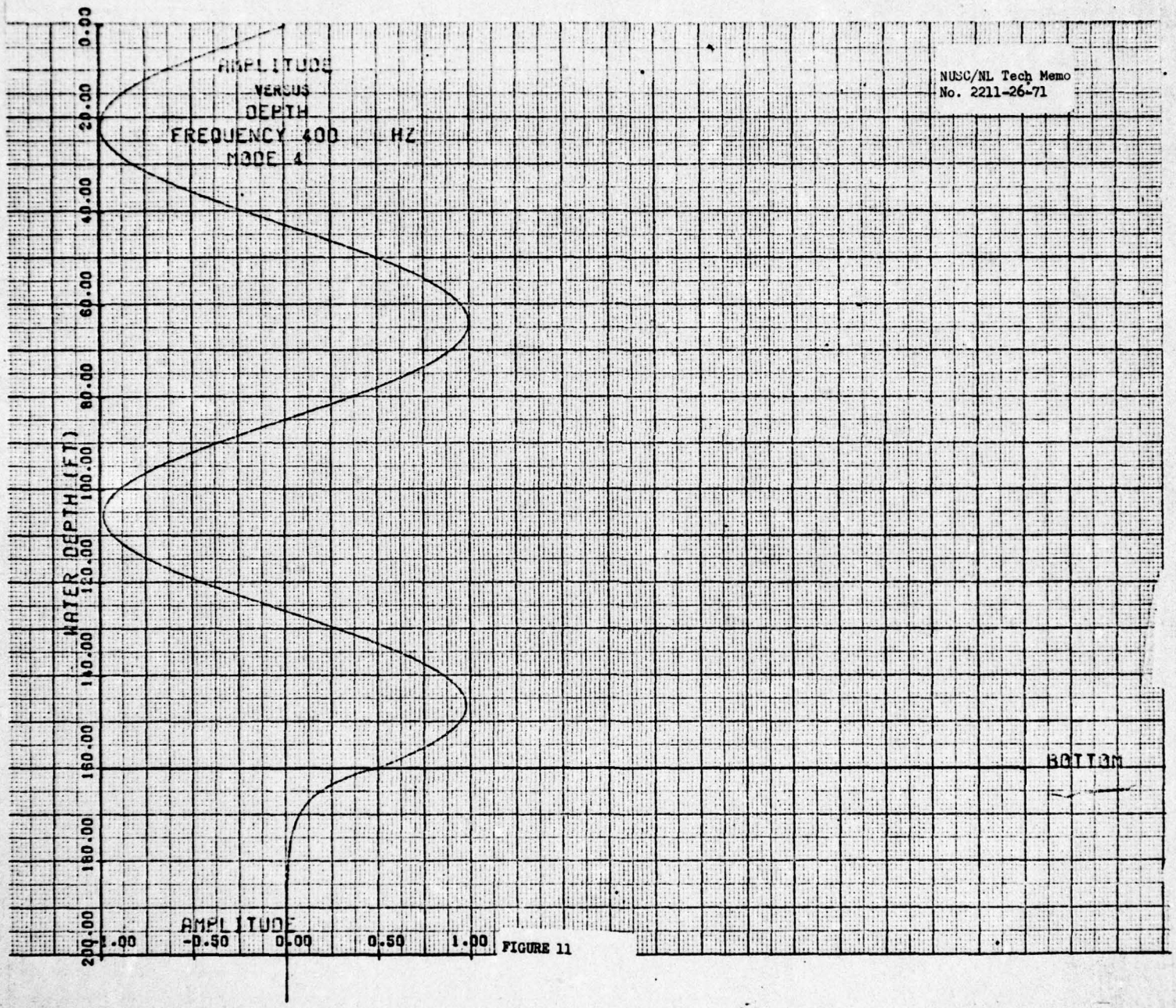

FIGURE 11

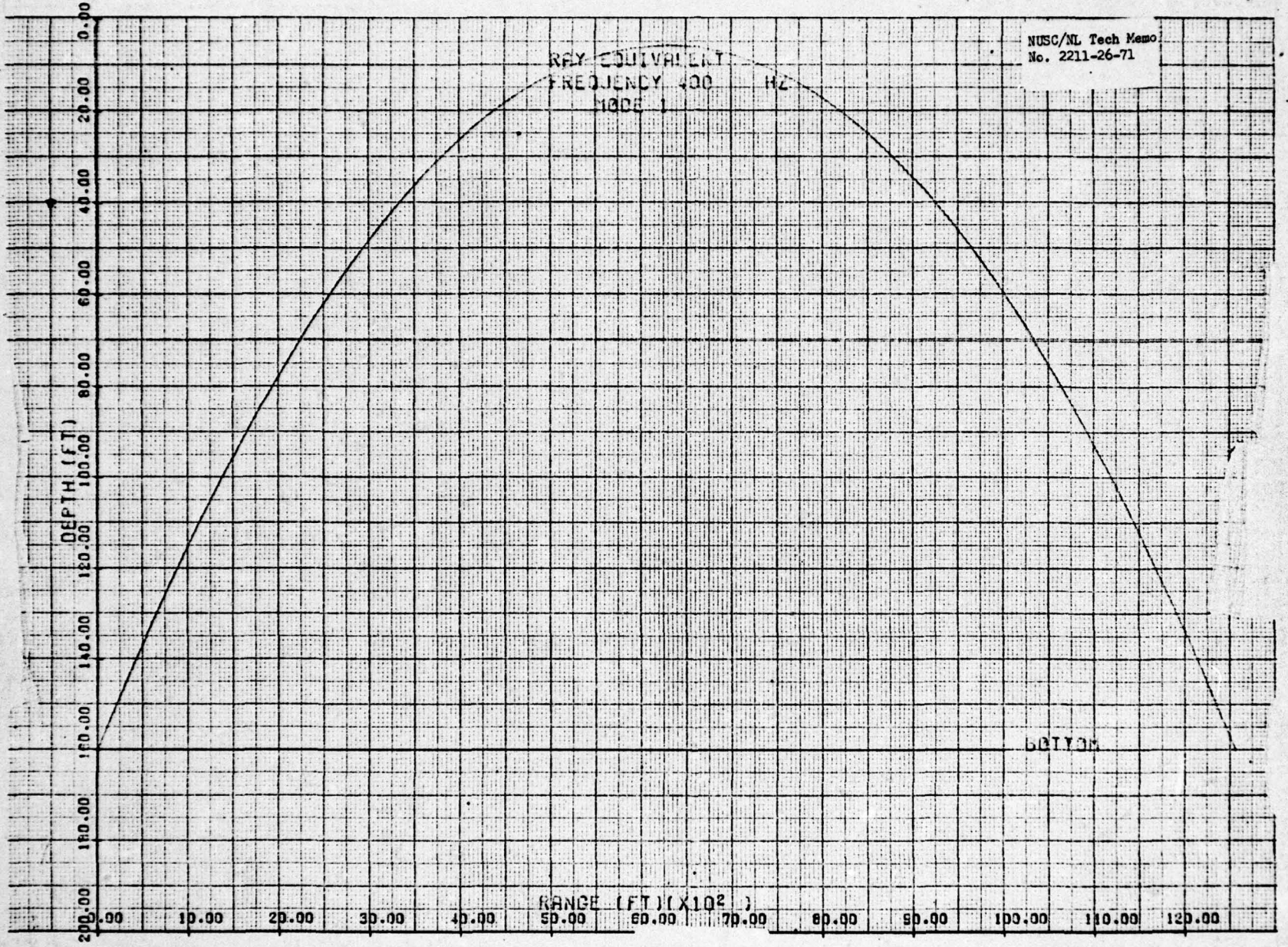

FIGURE 12

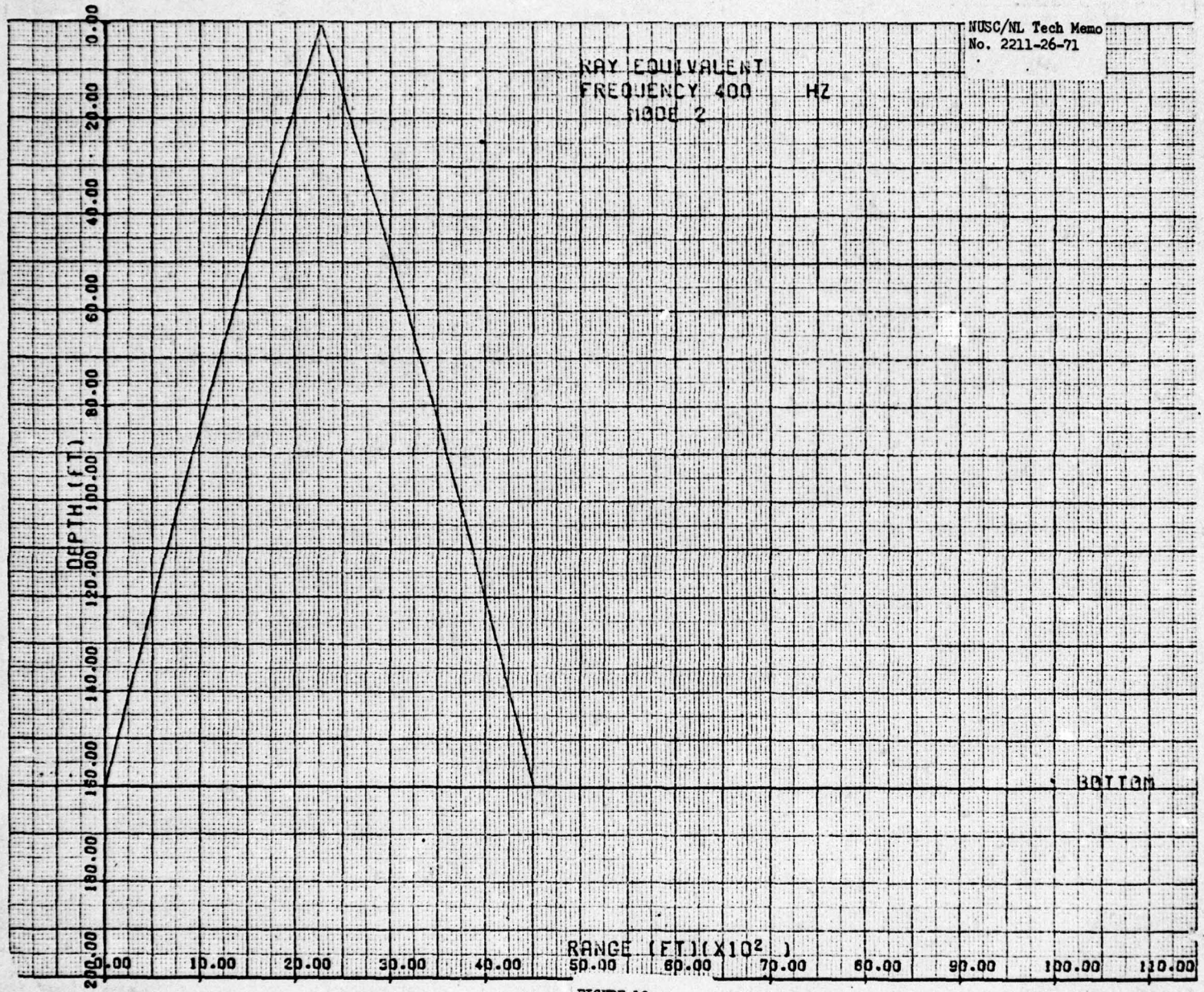

FIGURE 13

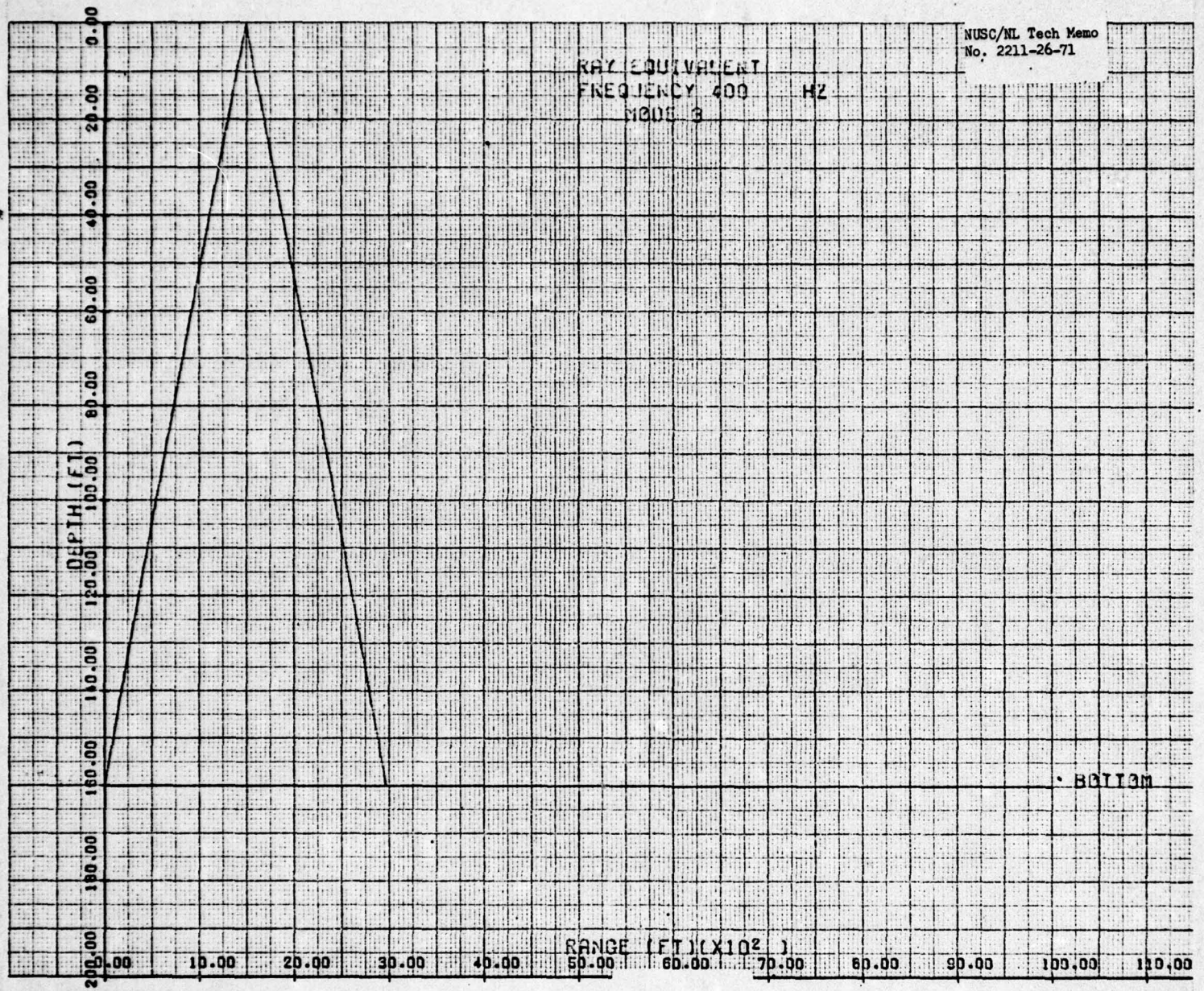
NUSC/NL Tech Memo
No. 2211-26-71
RAY EQUIVALENT
FREQUENCY 400 HZ
MODE 3
BOTTOM
DEPTH (FT)
0.00
20.00
40.00
60.00
80.00
100.00
120.00
140.00
160.00
180.00
200.00
RANGE (FT)(X10²)
0.00
10.00
20.00
30.00
40.00
50.00
60.00
70.00
80.00
90.00
100.00
110.00

FIGURE 14

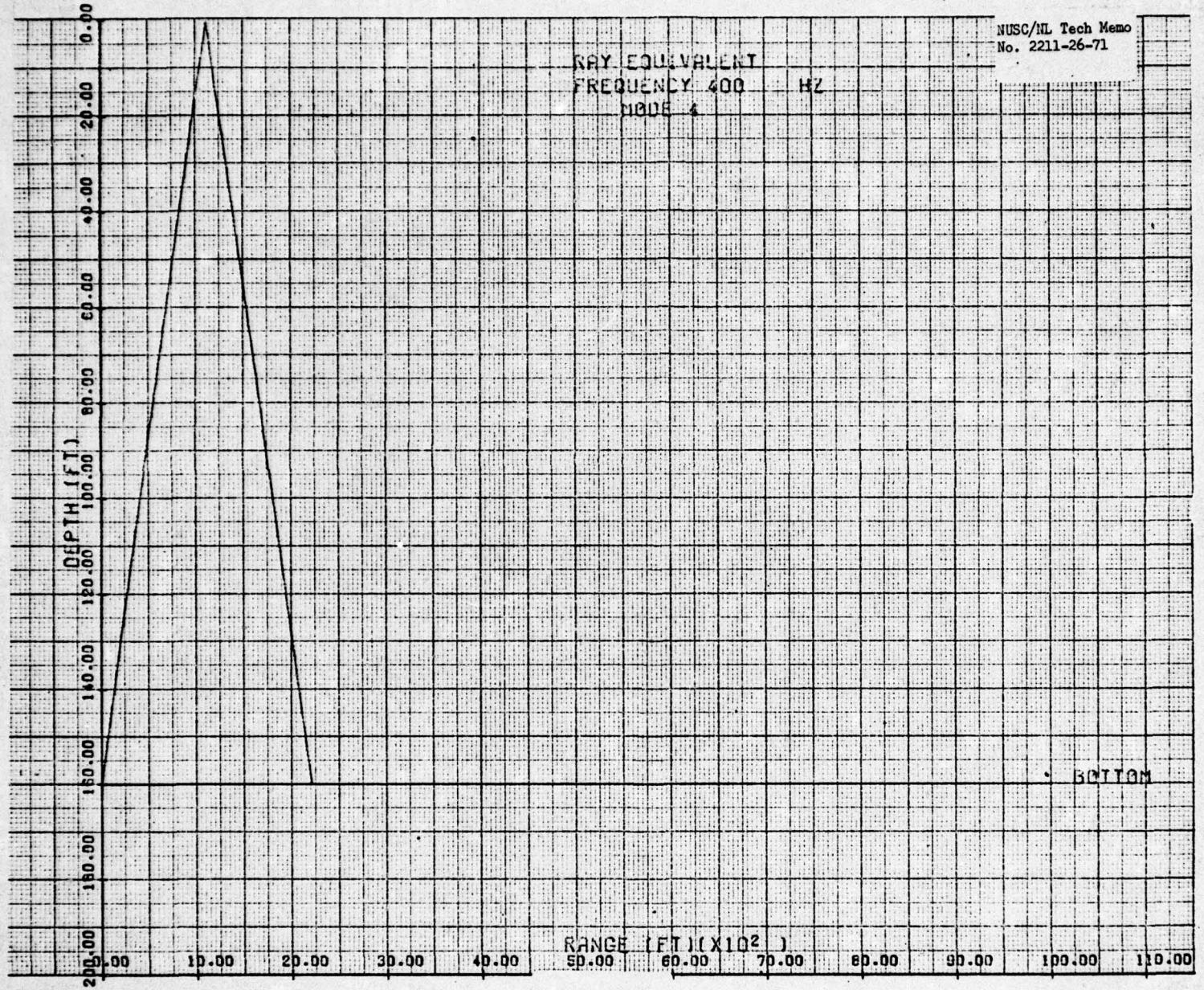
NUSC/NL Tech Memo
No. 2211-26-71
RAY EQUIVALENT
FREQUENCY 400 HZ
MODE 4
BOTTOM
DEPTH (FT)
0.00
20.00
40.00
60.00
80.00
100.00
120.00
140.00
160.00
180.00
200.00
RANGE (FT)(X10²)
0.00
10.00
20.00
30.00
40.00
50.00
60.00
70.00
80.00
90.00
100.00
110.00

FIGURE 15

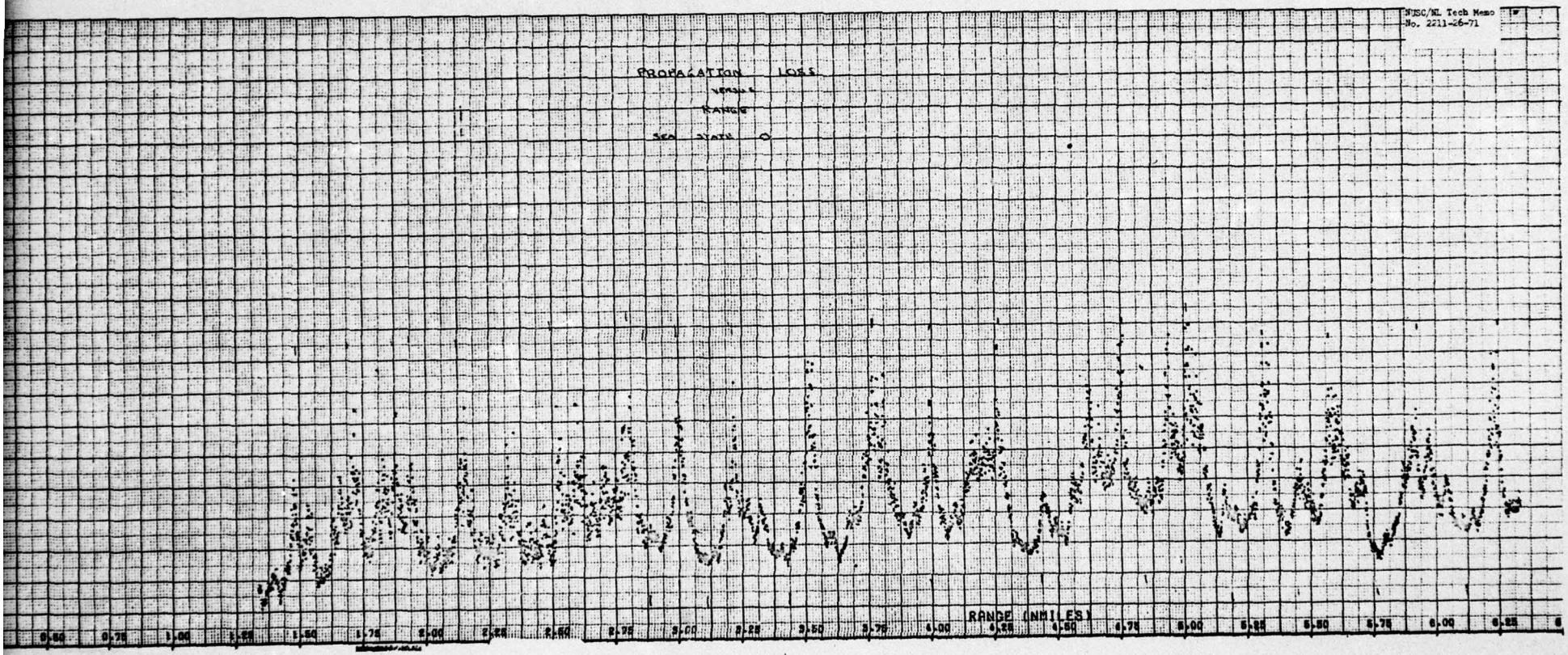

Fig. 16 - Propagation Loss vs. Range - Sea State 0

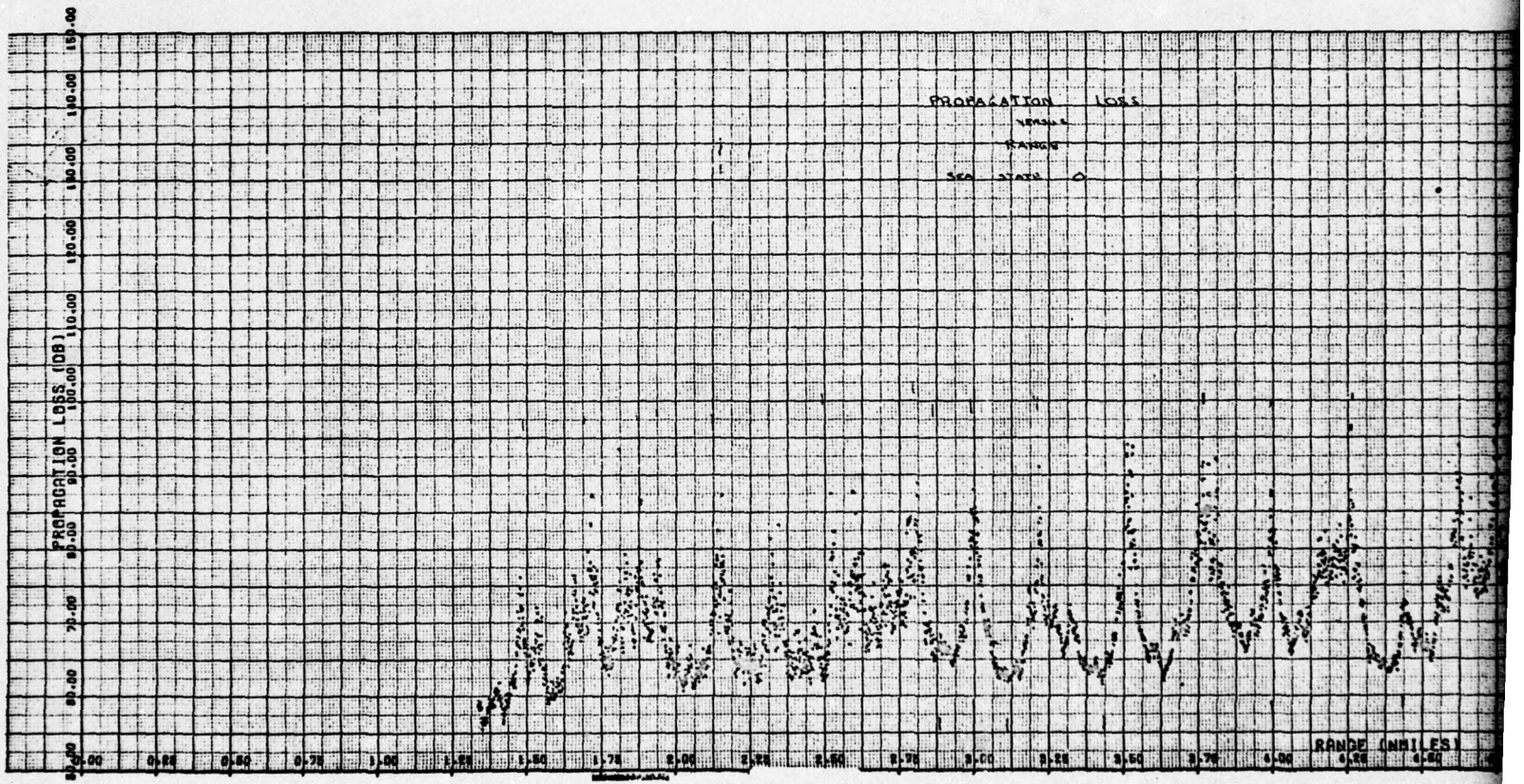

Fig. 16 - Propagation Loss vs. Range - Sea State 0

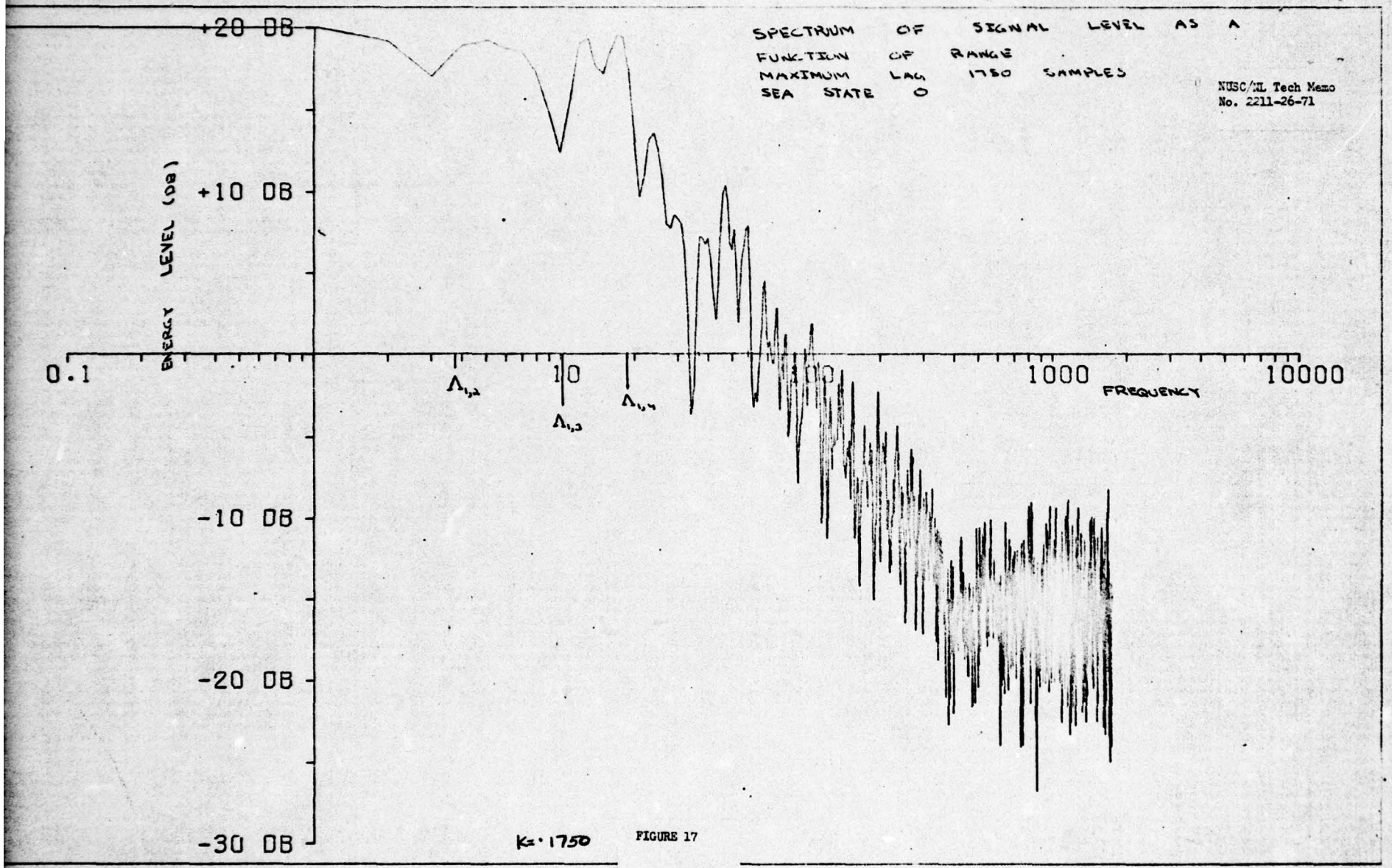
SPECTRUM OF SIGNAL LEVEL AS A FUNCTION OF RANGE
MAXIMUM LAG 1750 SAMPLES
SEA STATE 0
NUSC/NL Tech Memo No. 2211-26-71
+20 DB
+10 DB
-10 DB
-20 DB
-30 DB
ENERGY LEVEL (DB)
0.1
10
1000
10000
FREQUENCY
$\Lambda_{1,2}$
$\Lambda_{1,3}$
$\Lambda_{1,4}$
K=1750

FIGURE 17

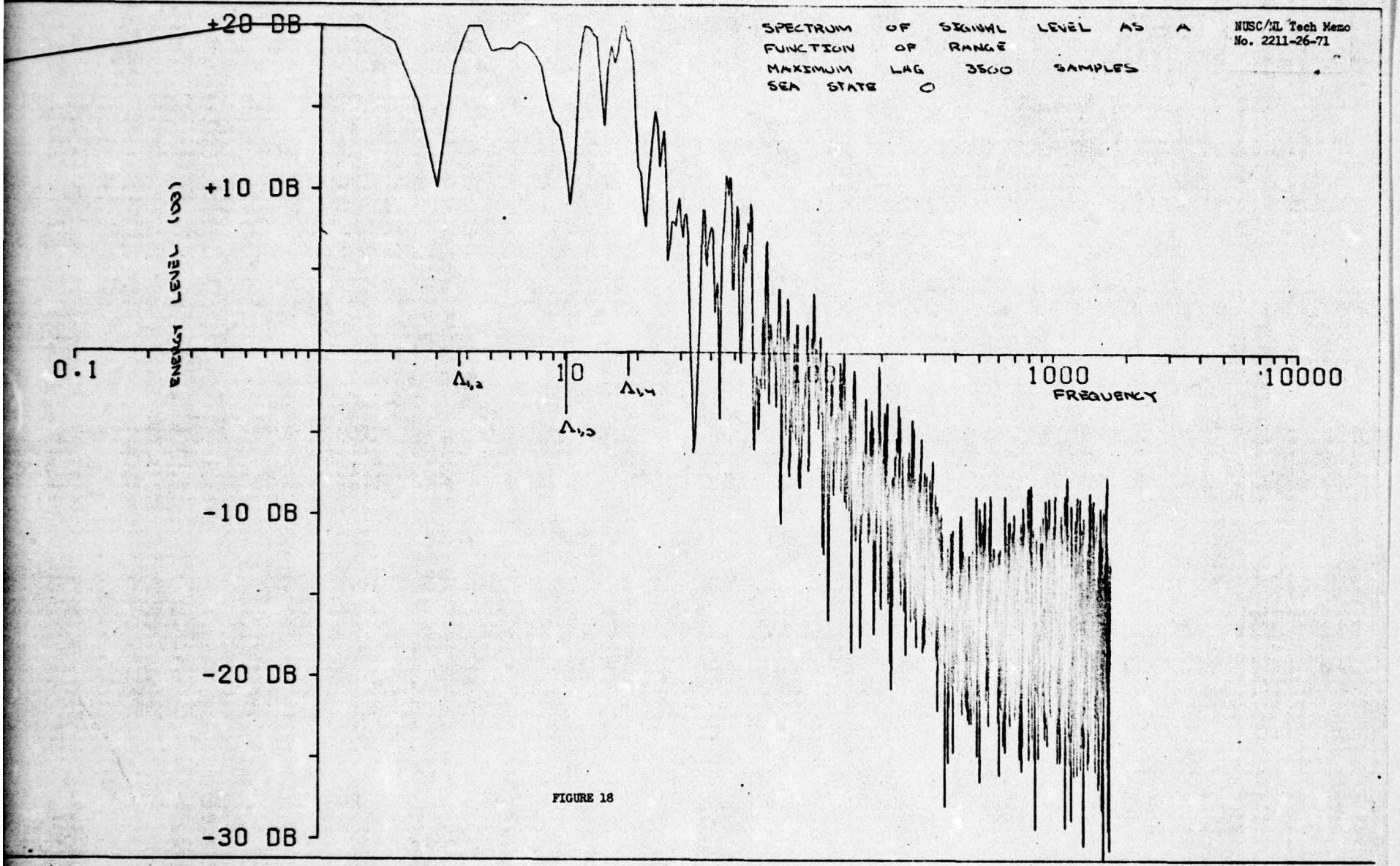

FIGURE 18

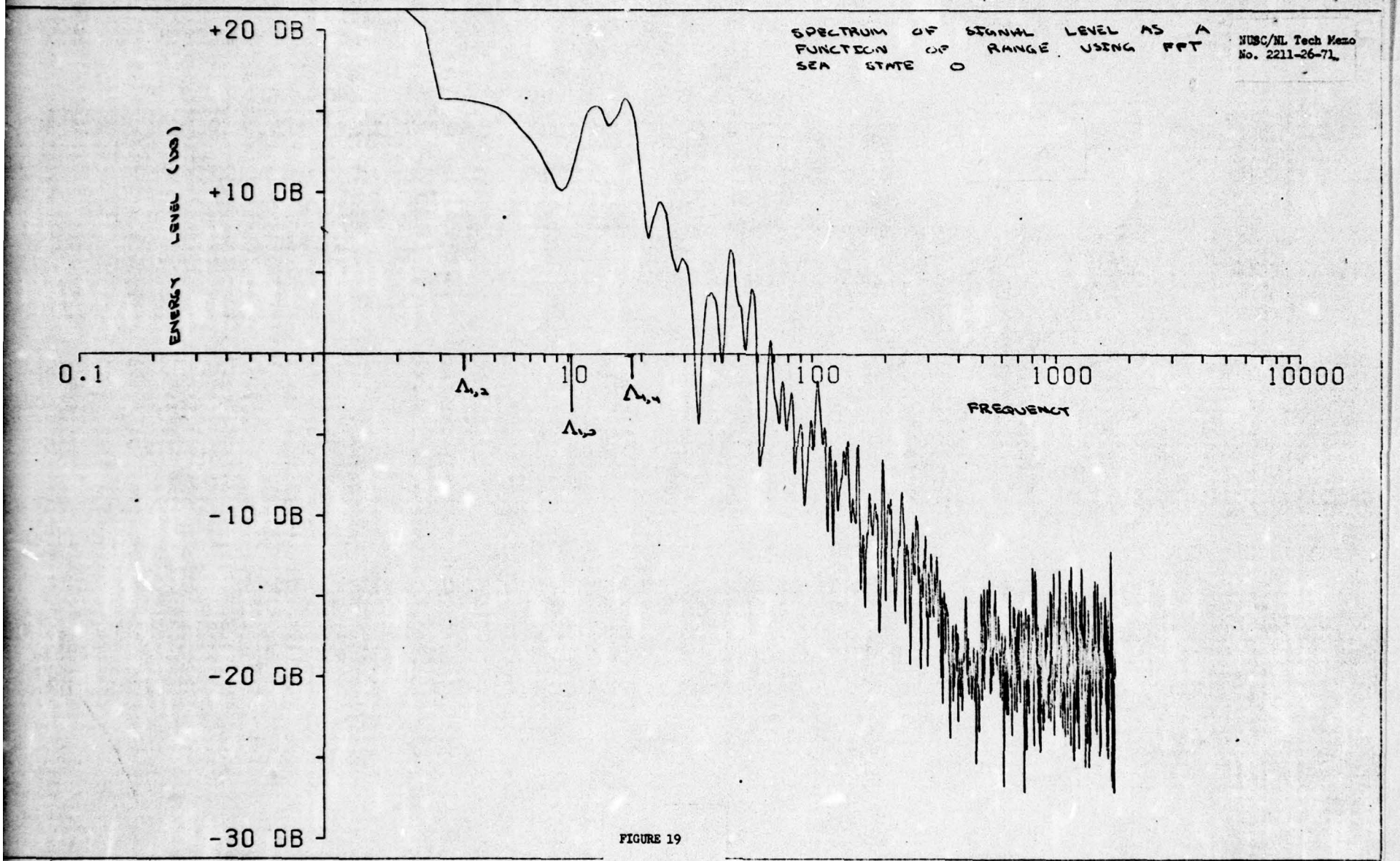

FIGURE 19

612 CALIFORNIA COMPUTER PRODUCTS, INC. ANA

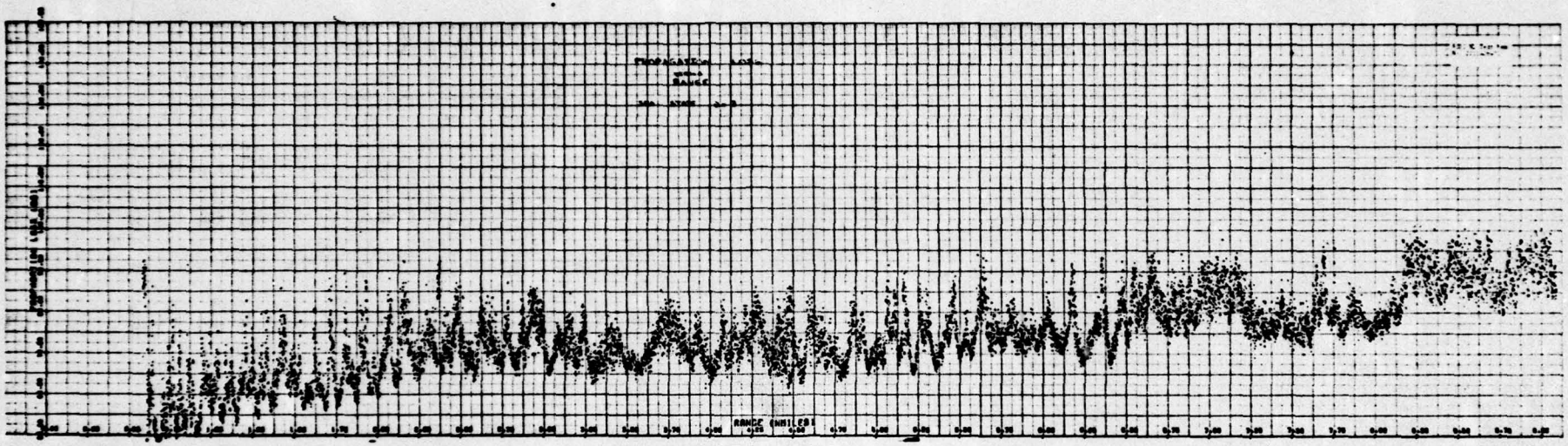

Fig. 20 - Propagation Loss vs. Range - Sea State 2 - 3

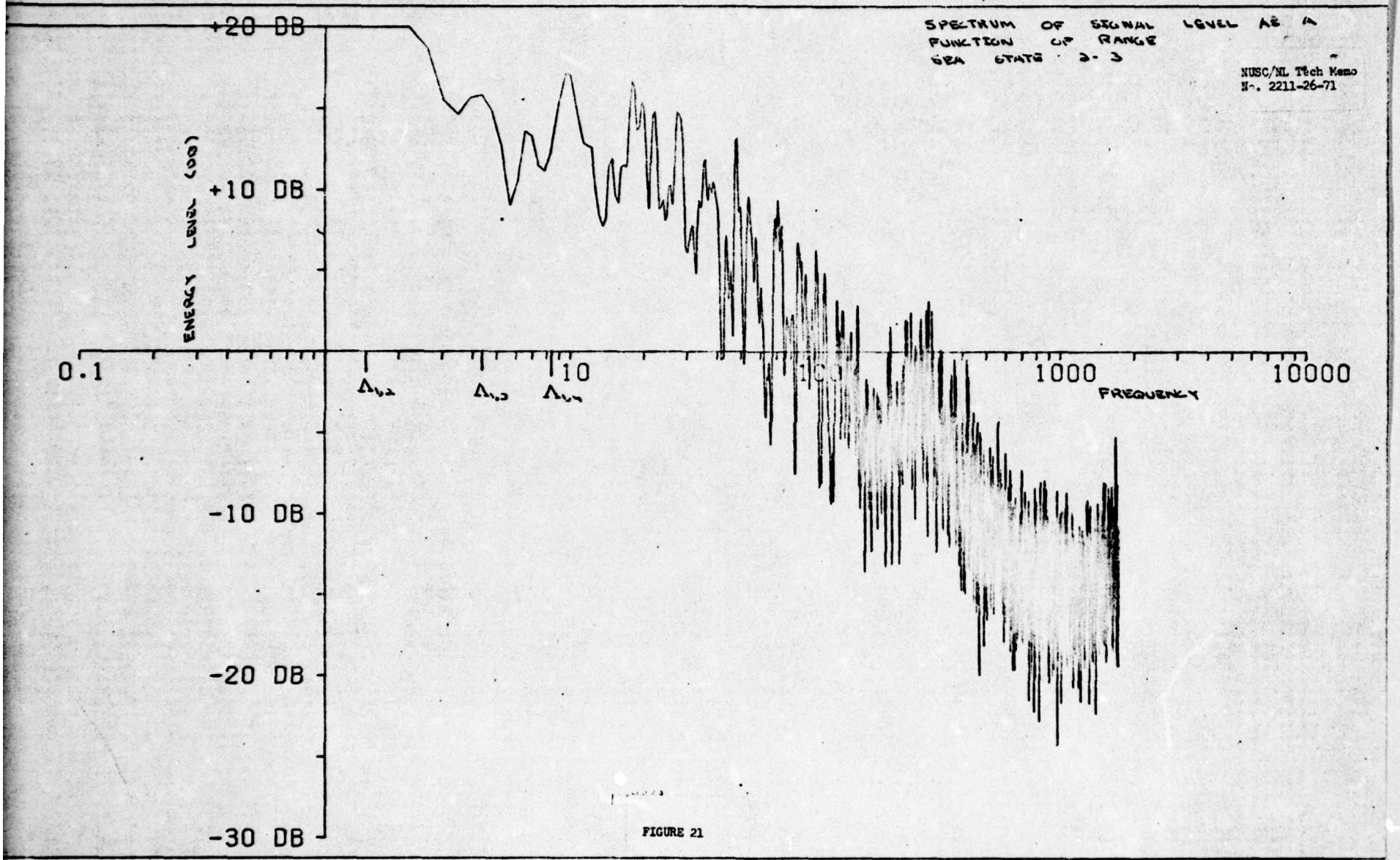
SPECTRUM OF SIGNAL LEVEL AS A FUNCTION OF RANGE
SEA STATE 2-3
NUSC/NL Tech Memo No. 2211-26-71
+20 DB
+10 DB
-10 DB
-20 DB
-30 DB
ENERGY LEVEL (DB)
0.1
10
1000
10000
FREQUENCY

FIGURE 21

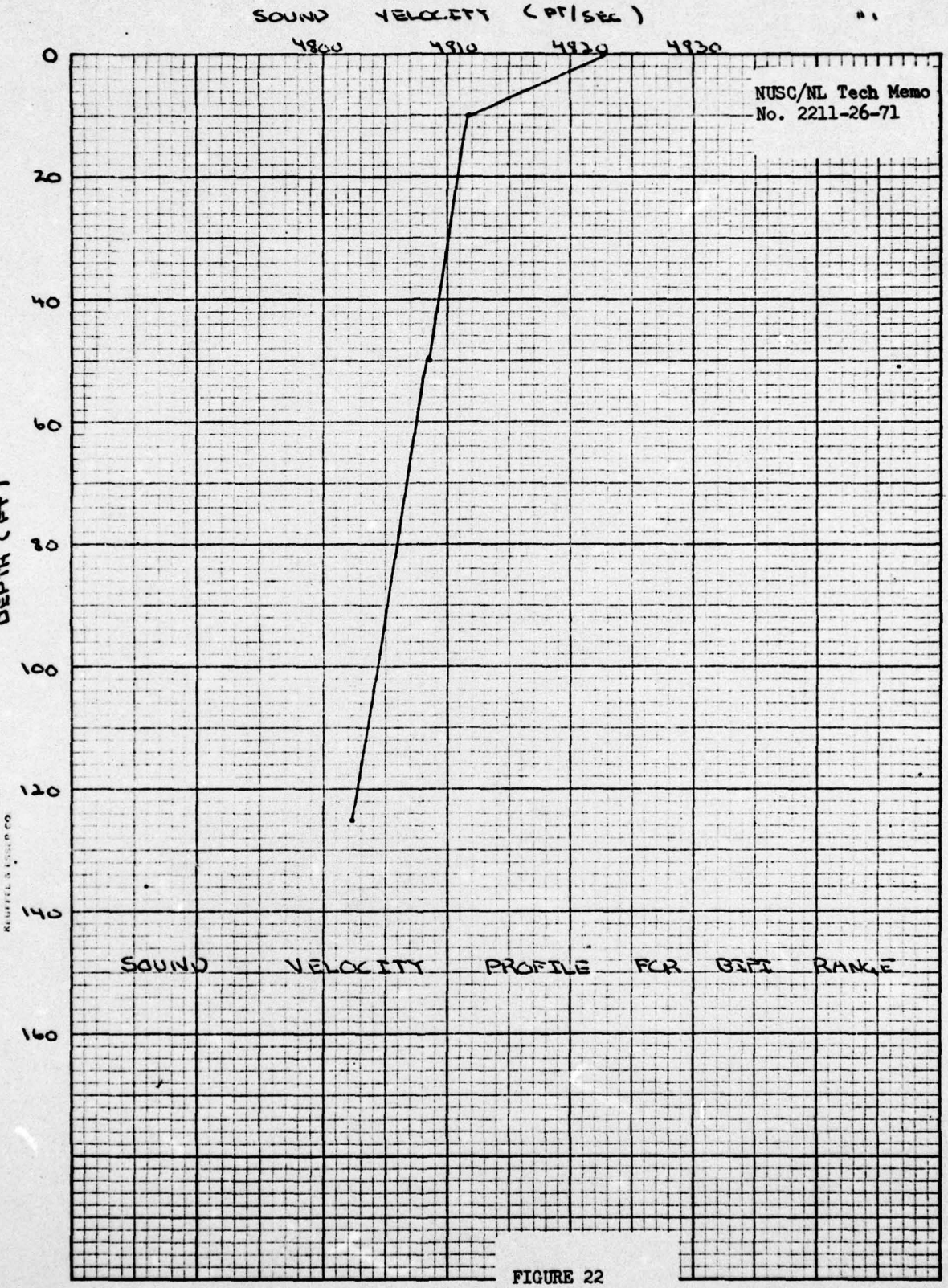
SOUND VELOCITY (FT/SEC)
4900
4910
4920
4930
0
20
40
60
80
100
120
140
160
DEPTH (FT)
NUSC/NL Tech Memo
No. 2211-26-71
SOUND VELOCITY PROFILE FOR BIFI RANGE

FIGURE 22

RECEIVED PULSE AT 400 HZ
SOURCE DEPTH 86 FEET
RECEIVER DEPTH 155 FEET

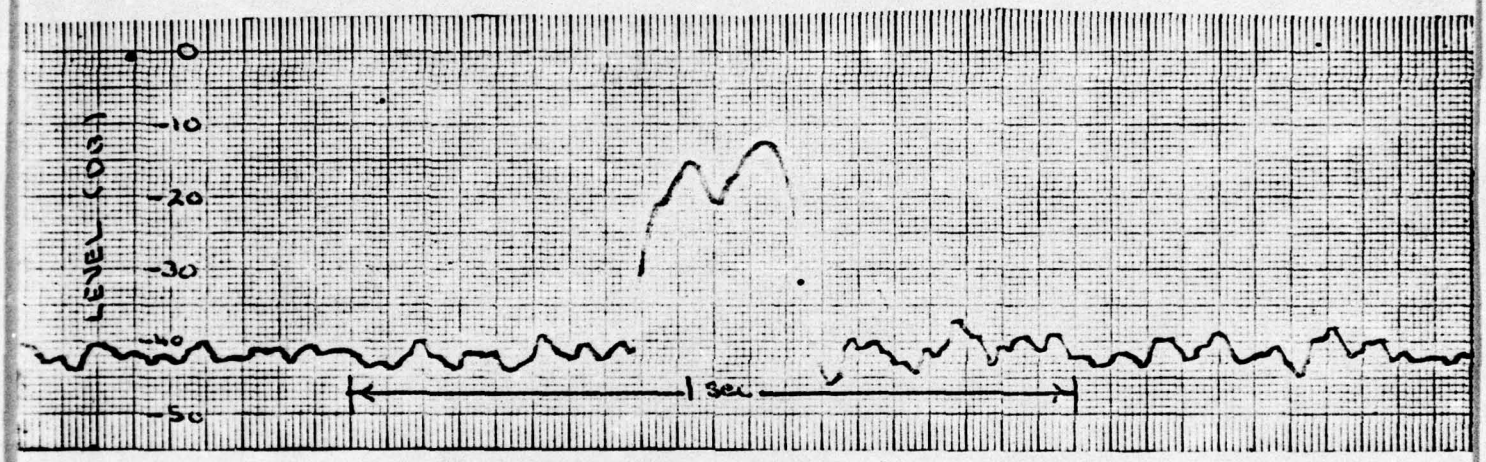

FIGURE 23

RECEIVED PULSE AT [illegible] Hz
SOURCE DEPTH 56 FEET
RECEIVER DEPTH 155 FEET

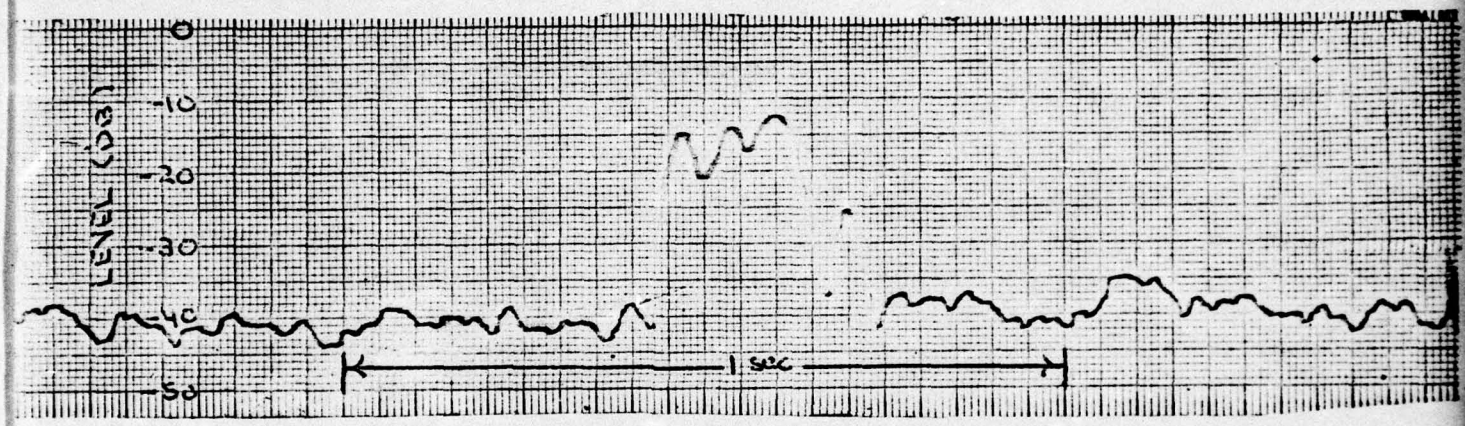

FIGURE 24